

Article

Adjusted Controlled Pass-By (CPB) Method for Urban Road Traffic Noise Assessment

Ricardo Moreno ¹, Francesco Bianco ², Stefano Carpita ², Alessandro Monticelli ³, Luca Fredianelli ^{1,*}
and Gaetano Licitra ^{4,*}

¹ Institute for Chemical-Physical Processes of the Italian Research Council, Via Giuseppe Moruzzi 1, 56124 Pisa, Italy

² iPOOL S.r.l., Via Antonio Cocchi 7, 56121 Pisa, Italy

³ Physics Department, University of Pisa, Largo Bruno Pontecorvo 3, 56127 Pisa, Italy

⁴ Pisa Department, Environmental Protection Agency of Tuscany Region (ARPAT), Via Vittorio Veneto 27, 56127 Pisa, Italy

* Correspondence: luca.fredianelli@ipcf.cnr.it (L.F.); g.licitra@arpat.toscana.it (G.L.)

Abstract: Noise associated with road infrastructure is a prominent problem in environmental acoustics, and its implications with respect to human health are well documented. Objective and repeatable methodologies are necessary for testing the efficacy of sustainable noise mitigation methods such as low noise emission pavement. The Controlled Pass-By (CPB) method is used to measure the sound generated by passing vehicles. Despite its popularity, the applicability of CPB is compromised in urban contexts, as its results depend on test site conditions, and slight changes in the experimental setup can compromise repeatability. Moreover, physical conditions, reduced space, and urban elements risk confine its use to only experimental road sites. In addition, vehicle speed represents a relevant factor that further contributes to the method's inherent instability. The present paper aims to extend the applicable range of this method and to provide more reliable results by proposing an adjusted CPB method. Furthermore, CPB metrics such as L_{Amax} do not consider the travelling speed of the vehicle under investigation. Our proposed method can yield an alternative metric that takes into account the duration of the noise event. A hypothetical urban case is investigated, and a signal processing pipeline is developed to properly characterize the resulting data. Speed cushions, manhole covers, and other spurious effects not related to the pass-by sound emissions of ordinary vehicles are pinpointed as well.

Keywords: urban noise monitoring; environmental acoustics; road traffic noise; sustainable mitigation; Controlled Pass-By; road elements noise; low-noise surfaces; electric vehicles



Citation: Moreno, R.; Bianco, F.; Carpita, S.; Monticelli, A.; Fredianelli, L.; Licitra, G. Adjusted Controlled Pass-By (CPB) Method for Urban Road Traffic Noise Assessment. *Sustainability* **2023**, *15*, 5340. <https://doi.org/10.3390/su15065340>

Academic Editors: Guillermo Rey Gozalo, David Montes-González and Antonio D'Andrea

Received: 29 January 2023

Revised: 7 March 2023

Accepted: 14 March 2023

Published: 17 March 2023



Copyright: © 2023 by the authors. Licensee MDPI, Basel, Switzerland. This article is an open access article distributed under the terms and conditions of the Creative Commons Attribution (CC BY) license (<https://creativecommons.org/licenses/by/4.0/>).

1. Introduction

While not the most annoying among the sounds emitted by transport infrastructures, roads are widespread and reach a great number of people in a capillary way. In 2019, 113 million Europeans were affected by noise levels greater than 55 dB(A) of L_{den} (day–evening–night level) [1]. In particular, at least 20% of the EU population was exposed to Road Traffic Noise (RTN) levels sufficiently high to induce long-term effect on health. In fact, even if it is very unlikely that long-term exposure to RTN would reach levels associated with risk of hearing loss [2], tinnitus [3], and hyperacusis [4] (>85 dB), the scientific literature has proven how long-term exposure to low–medium levels (45–65 dB) is followed by a variety of non-auditory health effects [5,6]. Among the most important and widely studied are cognitive impairment [7], behavioral and emotional disorders in children and teenagers [8], annoyance [9], sleep disturbance [10], depression and anxiety [11], hypertension [12], endocrine imbalance and cardiovascular disorders [13], and stronger physiological stress reactions [11]. Moreover, noise has been recognized as among the leading risk factors for cardiovascular morbidity and mortality worldwide [14].

It is therefore understandable how, in recent decades, many studies and research projects have been dedicated to investigating the phenomena of RTN generation for both indoor and outdoor [15] metrics in order to mitigate citizens' exposure [16]. The importance of research in this area is confirmed by an increasing number of studies on urban soundscapes [17] and the well-being of exposed people. Green and quiet areas [18] are all "traffic-free" solutions resulting from investigations into acoustic climate and mobility [19] and regeneration plans for urban areas [20].

The way in which a vehicle emits sounds depends on its speed. Engine noise is dominant for passenger vehicles below 30 km/h or heavy vehicles below 75 km/h [21,22]. Tyre/road interaction becomes dominant at higher speeds; its sound generation mechanisms are multiple, simultaneous (stick-slip, stick-snap, tread impact, and air pumping), and are amplified by the horn, Helmholtz resonance, and pipe resonance effects [23,24]. Different studies have been dedicated to separate these contributions and to investigate the frequency ranges of noise emitted by a running car [25–27]. While traffic flow, average speed, and car fleet age are non-negligible factors that influence the sound power level of a road stretch, the most important factors where it is possible to develop mitigation are the properties of the tires and pavement. In addition, surface features such as macro- and mega-texture, porosity, and layer thickness all play a key role in rolling noise generation [28,29]. Their relevance is expected to increase even further with the foreseen diffusion of electric vehicles [30,31], which have reduced engine noise in the low speed range and higher audibility of tire/road contribution. In 2021, the number of Electric and Plug-in Hybrid Electric Vehicles (EVs) in the European Union was about 4 million [32], with exponential evident growth in the last fourteen years. While EVs show reduced sound emissions from traffic noise at low speeds, the reduction is not evident between 30 km/h and 120 km/h, where rolling noise [33] is dominant. In fact, different studies have shown how traffic composition reduces overall exposure by no more than 2–4 dB(A) if not combined with silent tires and low-noise pavement [34–36]. For this reason, low-noise pavement is being chosen more often as a mitigation action [37,38] thanks to its positive effect on more citizens as compared to receiver-oriented solutions. Open-graded pavement, rubber asphalt, and poroelastic surfaces have proven to be consistent reducers of road sound emissions [39,40].

Both tyre and pavement noise have finally received proper attention at the community level for prevention of sound emissions. Today, tires have a specified noise label that describes their acoustic properties, and pavement has a minimum environmental emission level fixed by the EU Green Public Procurement Criteria (GPP) [41]. As the evaluation of new pavement noise emissions has become mandatory, measurements have become more and more relevant. The literature shows different methods of researching tyre/road interaction noise, with certain approaches being more source-oriented than others. The Close Proximity Index (CPX) ISO 11819-2:2017 [42] is the method most commonly applied to evaluate the GPP requirements. This method uses multiple runs of a test vehicle equipped with standard tyres measured by microphones placed close by. CPX can evaluate the pavement noise emission along its full length, and is able to identify pavement damage [43–45].

Another similar technique for analyzing the relative influence of pavement properties on tire–road noise is Behind-The-Tire (BTT) microphones. The BTT method provides good performance in the data acquisition stage for further identification of the actual condition of roads [46].

In the other hand, sound produced by real vehicle flow is measured using the Statistical Pass-By (SPB) method according to ISO/DIS 11819-1 [42] or consequent adaptations [47–49]. This assessment is based on roadside noise and traffic measurements. SPB is used to prove noise mitigation effects, as well as to study and refine useful parameters for noise propagation models. Pass-by measurements analyze sound generation and propagation of this energy for direct comparison with noise models. In the standard pass-by procedure, a microphone is placed 1.2 m above the ground and 7.5 m away from the center of the roadway. The time history of sound levels is acquired when individual vehicles pass by. Each event is considered valid only if a 10 dB(A) drop from the maximum level can be

found. The maximum level of this single event is the indicator used by the procedure, and is proportional to the vehicle speed according to a log-linear function. This should be valid under the assumption of a constant speed with the same vehicle and pavement. As such, the procedure requires the careful acquisition of speed data. During data processing, linear regression is then calculated using the best fit, and its outcome is the result estimated at the reference speed. The SPB method applies a data acquisition and processing protocol to freely circulating vehicles, with considerable data variability due to the variety of vehicles and driving behaviors. The Controlled Pass-By (CPB) method using NF S31-119-2:2000 [50] applies the same protocols to a vehicle driven in a controlled manner by trained personnel. Although the obtained result is less representative for the real vehicle fleet, it is not affected by the variability of the acquired data. CPB requires higher precision and robustness with smaller data samples. Moreover, its outputs are more reproducible and comparable with others obtained using different pavement or in different periods.

Nevertheless, CPB is not problem-free, and its applicability at every site or condition is not possible. In Section 2 of this work, we discuss the difficulties arising in the scientific literature around the applicability of the CPB method, together with several experimental issues resulting from our own experience. Subsequently, in Section 3, an Adjusted CPB method is developed to solve these issues. Finally, in Sections 4 and 5, the results and their associated uncertainties are thoroughly discussed and interpreted to provide an exhaustive overview of the adjusted CPB methodology.

2. CPB Issues

Despite its versatility and efficiency in controlled environments, the CPB method has shown a number of critical issues, mostly due to technical difficulties related to the conditioning of the highly controlled environment required for road measurements. This section reviews the issues that have been reported in the scientific literature, along with our own direct experience. Next, we explain adjustment procedures for CPB evaluation that can be developed in order to provide more reliable results.

While addressing the effective robustness of the results obtained through pass-by methods, Clar-Garcia et al. [51] noted that CPB measurements can be strongly influenced by external conditions such as the age or roughness of the pavement. For this reason, a slight change in the experimental setup may lead to significantly altered and non-reproducible results. They noted that CPB measures lack repeatability, even when the procedure is conducted by the same team and test vehicle. Despite the introduction of correction coefficients for well-known environmental variables such as temperature or humidity, other factors that are difficult to describe through weighting coefficients, such as wind speed, tire wear over time, and the effects of the surrounding urban soundscape, can alter the results of CPB measurements [51,52].

Ji et al. [53] pointed out excessive length of the measurement cycle and experimental costs as issues for the CPB method, and additionally reported that it may not be possible to obtain accurate and stable noise spectra through the CPB method in all certain circumstances due to the unavoidable influence of the surrounding acoustic environment.

In 2016, using measurements from the Leopoldo Project, Licitra et al. [54] highlighted the limitations of the procedure's SEL_{10dB} metric for noise assessment. According to the definition in [42], the distance needed to observe a 10 dB decrease in signal intensity depends on the vehicle's speed according to a power law. Due to the susceptibility of the CPB method to external condition, this might lead to unreliable results. Furthermore, the evaluated road length is dependent on the overall condition of the pavement. These observations suggest that SEL_{10dB} measurements should then be carried out on variable distances according to the vehicle speed.

Thus, the presence of unevenness can compromise the stability of measurements carried out with the CPB method and characterized through the SEL_{10dB} metric. Real measurement sites that present road distress or unevenness are common. Unfortunately, SEL_{10dB} -based CPB analysis can only yield rigorous and reproducible results in a selected

and restricted number of cases, for example, on smooth road pavement with constant monitoring of tire and vehicle conditions. The pavement may present several kinds of unevenness, including road deterioration such as severe road cracking, potholes, presence of stripping or raveling of the surface, and raised asphalt patches, as well as the presence of structures usually found in urban areas, such as manhole covers or speed bumps, which cannot be fixed through road maintenance operations.

Other studies [43,54] have compared the pros and cons of the CPB method related to other frequently employed noise assessment methods, such as the CPX method. Another method, the near field technique, allows for labeling, controlling, and validating the wear course using a mobile laboratory. It is not suited to evaluating pavement distress, however, due to the chance of damaging the instrumentation. The acoustic contributions of pavement distress are not very well identified, as impulse components destroy the rest of the frequency response contributions. This measuring technique can provide invaluable information for source-specific noise pertaining to rolling. However, it is not sufficient to yield a faithful description of road traffic noise in an urban environment, as it does not take into account the contribution of engine noise. Meanwhile, CPB/SPB methodologies provide information on the overall vehicle noise as well as its propagation. These studies stress the importance of a rigorous definition for both the CPX and the CPB indexes, and when used jointly they can provide a truthful description of the environment under investigation.

In the context of the present work, special attention was devoted to a particular application of the CPB method to road pavement performance assessment. In fact, the CPB method is widely used to evaluate the effective acoustical behavior and efficiency of low-noise surfaces for speeds higher than 60 km/h.

Hence, providing information about the acoustic properties of a certain pavement implies measurements that must be conducted on-site, where it might not be possible to obtain the controlled conditions required for application of the standard CPB protocol. The problems inherent to the method cannot be solved through on-site intervention to grant favorable conditions. Therefore, it is necessary to develop a more stable approach to CPB measurements in order to apply this method to investigation of the acoustic performance of low-noise road pavement.

For CPB measurements, the National French Standard (NF S 31-119-2) specifies a method using a microphone at the position detailed above [50]. Nevertheless, this procedure is structured in such a way as to measure the acoustic emissions of tire-road interaction during passage at speeds faster than 60 km/h, which requires a longer free field and a more controlled environment. Measurement conditions require a very long segment of road of at least 40 m, plus the distance for the vehicle to reach the desired speed, and another 10 m to 50 m radius area around the microphone must be free of obstacles. In this context, measurement in urban situations means more restrictions and less controlled conditions.

According to our own direct observations, the CPB protocol performed in the vicinity of a site with a hypothetical morphology similar to that presented on the left side of Figure 1 would be compromised by the presence of citified elements. In this scenario, a speed cushion and a pedestrian crossing, which are commonly installed in crossroads and T-intersections, are depicted after the region of interest in front of the measurement station. These elements are indicated in blue and red, respectively. Other kinds of road unevenness, such as manhole covers, which can further disturb the data, are represented in yellow. The right side of Figure 1 reports the correspondent signal acquired at the measurement station during a pass-by. Driving over a manhole cover contributes additional sound energy that is not directly related to the tire-road interaction noise. This additional contribution depends on the quality of the finishing between the pavement and the iron lid. In general terms, the presence of these urban elements represents a major issue for signal acquisition and post-processing of the data. This noise contribution, which is proportional to the vehicle speed, causes deviation of the noise estimation, reducing the dynamic range and creating other peaks not related to the passing-by. As a result, effects other than those caused by the passage are clearly evident in the recorded signal.

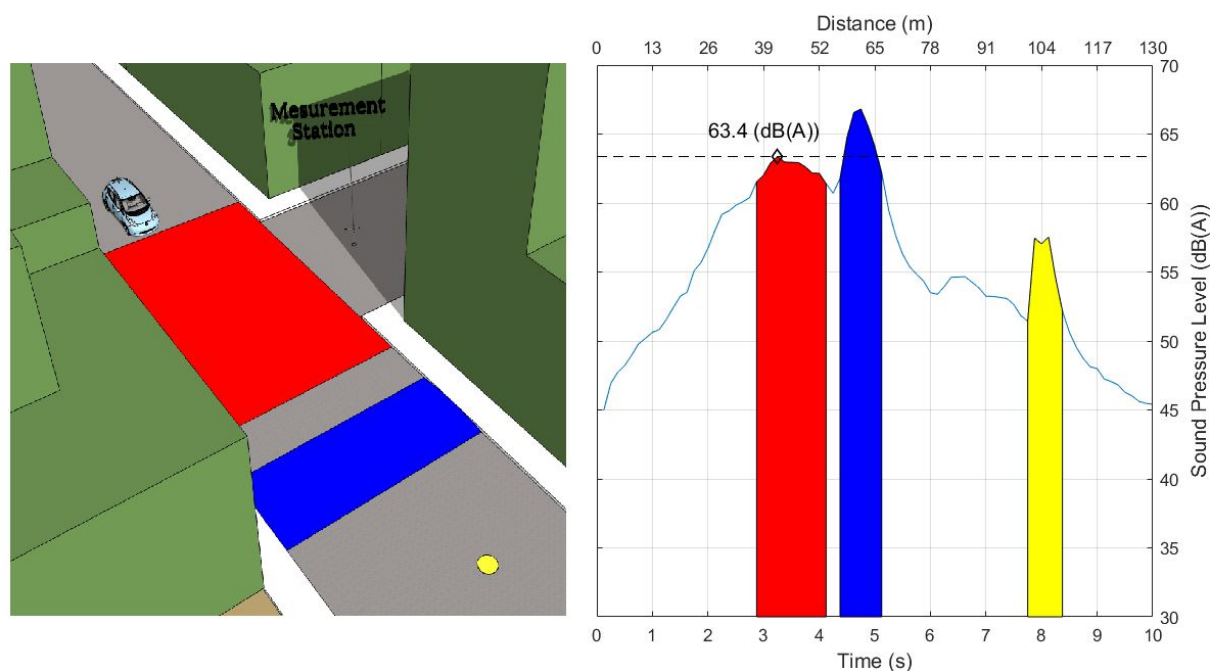


Figure 1. Example of a speed cushion and a manhole cover effects in the proximity of the pavement under investigation. The red region corresponds to the road segment of interest. Blue and yellow portions are related to the noise produced by the vehicle driving over a speed cushion and a manhole cover.

The primary red peak, around the 3 s and 15 m length, is associated with the passage of the vehicle under examination. In the vicinity of 5 s mark, a peak highlighted in blue corresponds to the vehicle driving over a speed cushion. Lastly, a third peak associated with the interaction between the vehicle and the manhole cover is visible around 400 ms. In addition, two peaks can be noticed, which respectively correspond to the front and rear wheels falling into the manhole-cover.

Projects such as HARMONOISE have developed and validated methods to assess traffic noise emission [47]. The IMAGINE project studied the discrimination of rolling noise subsources and their emissions [48]. The maximum A-weighted Noise Level (L_{Amax}) and Sound Exposure Level (SEL) were the metrics used to determine and model the noise emissions of tire-road interaction. Additionally, as explained in [24,50], L_{Amax} can describe acoustic emissions for speeds higher than 60 km/h.

In a free field and under controlled conditions, the closest point between the source and the receiver during a passage can coincide with the L_{Amax} sample position. However, in urban environments, obstacles may be present that can lead to the vehicle generating other peaks not related to the source while approaching the microphone. These other contributions can be occasionally louder than the passage itself, leading to the automatic recognition of the maximum level to be altered. These other noise contributions belong to the response of vehicle systems other than the rolling parts, i.e., when wheel compression is stressed by the bumper, it produces other kind of reactions in the damping system and a variation of the aerodynamic flow, which in turn means that measured energy contains information from the operation of other vehicle systems even if other noise events are not louder than the passage itself. At low speeds, the duration of the passage is a significant issue for assessing sound energy, and describing vehicle pass-by using this parameter is not sufficient. After the correct peak of the signal is identified, the sound energy can be evaluated by means of the exposure level, either L_{AE} or SEL . One of the reasons for calculating this parameter is to estimate the noise emission of the vehicle passage in one

second; the reference time is $T_0 = 1(s)$, where T corresponds to the time of evaluation, as in Equation (1).

$$L_{eq} = SEL - 10 \log\left(\frac{T}{T_0}\right) \quad (1)$$

Moreover, L_{eq} is used to estimate these events in terms of the number of vehicles (n) that pass in a given street, as expressed in Equation (2).

$$L_{eq} = 10 \log(n) + SEL - 10 \log\left(\frac{T}{T_0}\right) \quad (2)$$

Then, the SEL value can be calculated by determining a region of the signal. For this, a 10 dB threshold below L_{Amax} is employed to find two signal interceptions. Energy between the cutting points is integrated as shown in Figure 2.

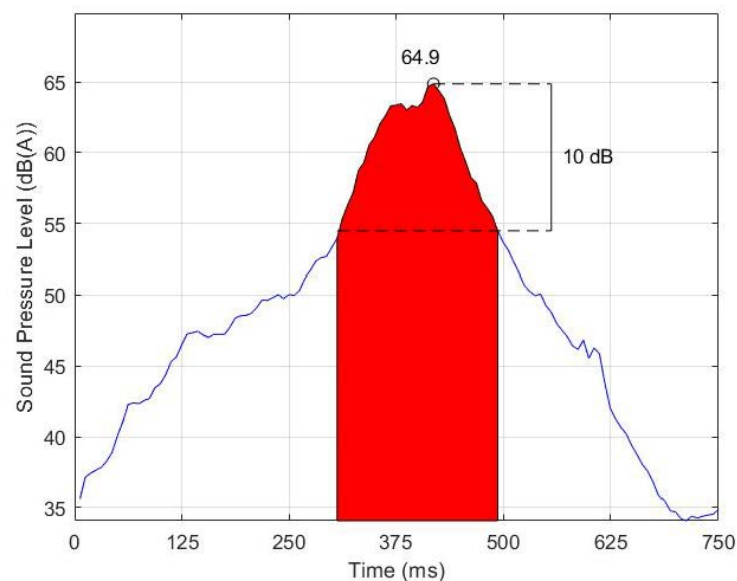


Figure 2. Example of a signal passage. The integration value of the red region corresponds to the Sound Exposure Level SEL_{10dB} . The duration of this region is determined by the threshold at 10 dB below L_{Amax} , indicated with a black circle.

This parameter is affordable when the background noise is quite stable and other noise contributions do not affect the fade-in and fade-out of the signal. Indeed, SEL_{10dB} can be calculated whenever the sound emission of the vehicle passing by is clearly producing more than 10 dB and driving is not affected by other road conditions that might force a maneuver. In short, a threshold of 10 dB means that energy events are not being affected by other noise contributions for at least 20 m before and after the center axis where the microphone is aligned.

3. Adjusted CPB Procedure

The present work defines a clear methodology that extends the range of applicability of the standard CPB procedure. An adjusted SEL index based on the road segment under evaluation and the vehicle speed is explained in this section. The new metric is obtained by means of CPB configuration under certain modifications. The same principle, that is, simultaneously acquiring the sound pressure level and speed while the vehicle passes in front of the measurement station, is contemplated in the adjusted procedure. The following subsections detail the required technical equipment, measurement conditions, signal processing, and expression of results of the new metric.

3.1. Equipment

The sound energy of passages is recorded in .wav files using a free field class 1 microphone. To avoid airflow produced by the vehicle run, windscreens are needed. If site conditions allow it, an optional second point on the opposite side of the street can be set up as well. For digital signal conversion, a module connected to a portable PC is considered for recording data. Signals must be acquired with a frequency sample high enough to analyze data in the third octave band without aliasing.

Equipment for measuring the speed of vehicles has to be verified by the manufacturer and calibrated. Calibration of pressure must be performed at the beginning and the end of the measurement. Calibration signals are recorded and used as a reference for pressure during post-processing.

The information about vehicle speed is of the utmost importance for correct application of the adjusted CPB procedure. Hence, traffic counters should be employed for providing reliable and accurate speed measurements on the test site. However, field measures for vehicle speed might not always be feasible. In these cases, speed models can represent a solution [55–57].

3.2. Measurement Conditions

The test vehicle is driven around the range of the speed limit in urban areas, i.e., 50 km/h. Repetitions can be considered at 45 km/h, 50 km/h, and 55 km/h. Passages speeds are distributed over the range of 20 km/h to 70 km/h in order to estimate a model of the noise emission, as detailed in Section 3.4. The trajectory of the vehicle must be delineated on the ground, as shown highlighted in pale blue in Figure 3. In this way, the driver can hopefully avoid any manhole covers or potholes. In addition, not conserving the center of the lane might modify the distance between the source and the receiver. Preferably, the evaluation segment should be entirely free of potholes, manhole covers, and/or speed cushions.

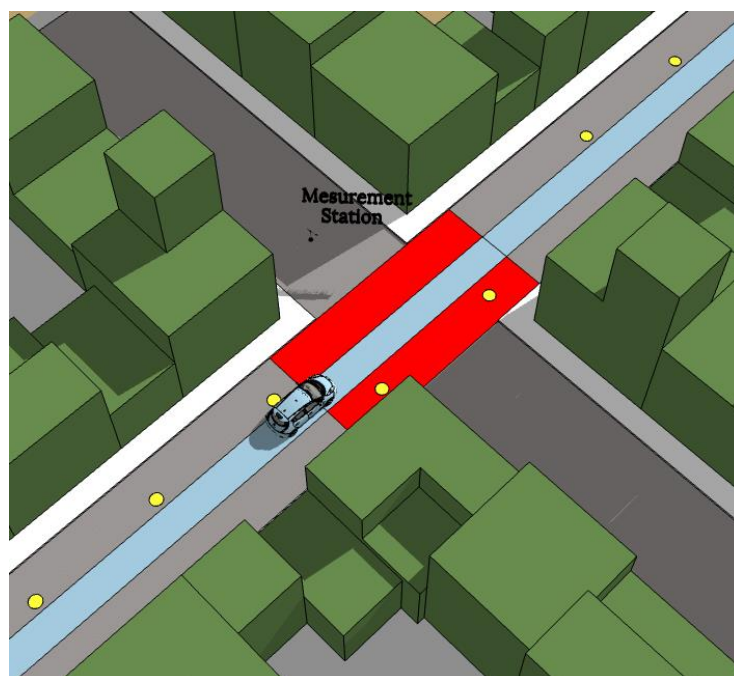


Figure 3. Delineated vehicle path for measuring session.

It is suggested that measurement stations be placed at crossroads (Figure 3) or T-intersections (Figure 1). The microphone position is 7.5 m from the center of the lane and at a height of 1.2 m from the ground. Because the proposed modification of the CPB method is meant to be applied in densely populated places, any façade reflections or

acoustic shadows of buildings must be outside a quarter-sphere with the radius being the microphone distance, as illustrated in Figure 4.

For security reasons and to ensure the quality of results, highly controlled traffic flow conditions and case-specific vehicle fleets have to be assured in order to comply with the CPB specifications. As general advice, the investigated road sections should be closed to vehicular traffic during the acquisition process.

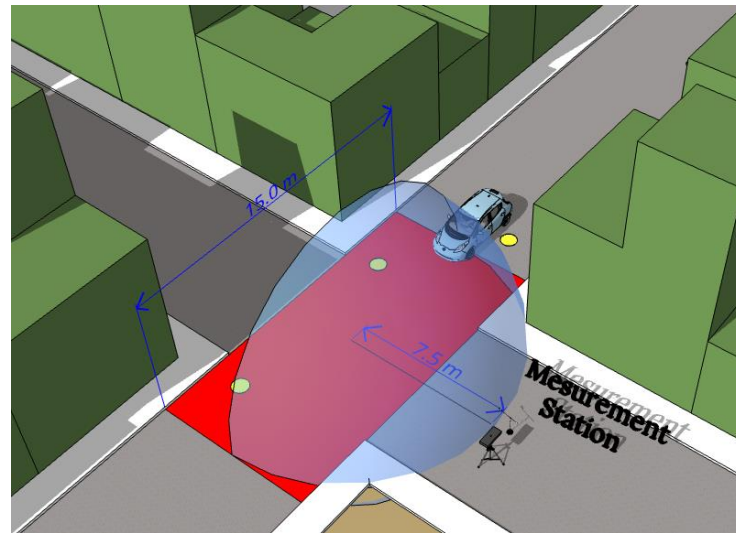


Figure 4. Microphone position and measuring conditions.

In addition, a segment of the road prior to the measurement region has to be considered to ensure that the vehicle reaches the desired speed. This distance is determined by the acceleration capacity of the vehicle. For instance, diesel internal combustion vehicles have an average of acceleration capacity (a) of 2.23 m/s^2 [58], while EVs can reach 6.1 m/s^2 . The minimum length needed of this segment of road (Δx) is determined by the speed of each passage (V) 20–70 km/h, and corresponds to the acceleration capacity of the vehicle under examination, as described in Equation (3) and Table 1.

$$\Delta x = \frac{V^2}{2a} \quad (3)$$

Table 1. Minimum road segment for acceleration.

Vehicle	Speed (km/h)	Acceleration Capacity (m/s^2)	Acceleration Segment Δx (m)
Internal Combustion	70	2.6	72.7
Electric	70	6.1	31.0

3.3. Signal Processing

Signals obtained through this pass-by methodology follow the flow diagram depicted in Figure 5. Data analysis is designed for processing data by session. In this way, the performance of different combinations of vehicle, tire, and asphalt can be registered for later performance comparisons or fleet evaluation.

As previously mentioned in Section 2, the presence of manhole covers and speed cushions can induce difficulties in the signal processing stage. Signals might have an irregular fade in and/or out, and this energy does not allow for more than 10 dB of dynamic range.

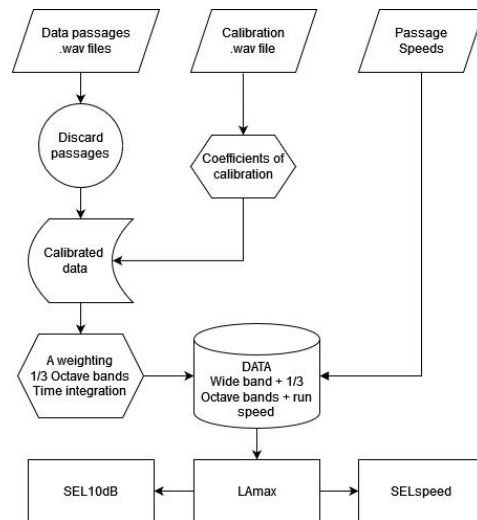


Figure 5. Flow chart of signal processing.

A vehicle passage is considered as an event with a duration that depends on its speed of travel. Low-speed passages allow the closest position to be estimated by means of the proximity effect of the sound pressure level. In fact, whenever the shape of the signal resembles a Gaussian function, this kind of model can be fitted in order to estimate the position at which the vehicle reaches the closest point to the microphone, as depicted in Figure 6. In addition, for open space without any obstacles, signals recorded at a test site with ideal conditions can be fitted with a single Gaussian function, allowing the direct sound to be registered and its approaching effect to be clearly defined. However, real test site noise contributions cannot be estimated with a high level of confidence interval. Therefore, a second Gaussian function should be applied to approximate the function to the noise energy, such as street canyon reflections and background noise, that is not related to the passage. Moreover, as the fitted model must be restricted to already-known signal characteristics, speed and region length values are used as bounds on it. For instance, both peak widths have to be proportionally adjusted to the rate between time integration, length of the road section, and speed of each passage. The amplitudes of both functions are useful for identifying direct sound and other contributions. As a result, the centroid position of the first Gaussian function establishes the closest point of the vehicle to the microphone, and the portion of the signal according to each speed passage determines the region of the signal to be integrated.

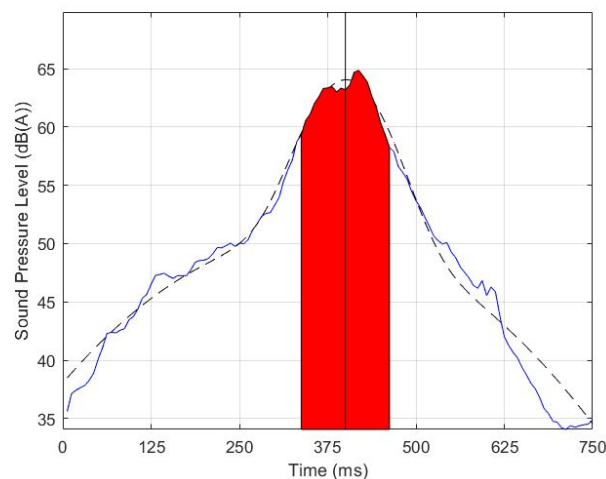


Figure 6. Cutting points for SEL parameters and L_{Amax} position.

The blue line in the figure corresponds to the time-integrated A-weighted signal, while the black dashed line indicates the double Gaussian fitted model estimated for a single passage and the centered vertical black line indicates the maximum point of the double Gaussian function.

Thus, SEL_{speed} can be calculated by integrating the energy within a temporal window adjusted by the time the vehicle takes to travel along a given segment of the road. As the distance between the microphone and the center of the lane is 7.5 m, the same distance after and before the closest point of the station is 15 m. Thus, an angle of 45 degrees exists at the beginning and end of the 15 m region. To integrate the noise energy of each passage, the size of the temporal window is calculated; the number of samples depends on the speed, segment length, and integration time of the signal. Table 2 shows the size of the window when the signal is acquired with “fast” integration (125 ms) and over a 15 m segment.

Table 2. Window size of SEL_{speed} .

Speed (km/h)	Duration (s)	Samples (n)
20	2.7	22
30	1.8	16
40	1.4	12
50	1.1	10
60	0.9	8 ¹
70	0.8	8 ¹

¹ Due to rounding, the fastest run speeds are not less than 1 s in duration.

Furthermore, the estimation of the temporal window integrates the energy symmetrically, and only even numbers are used. In addition, the number of samples (n) is rounded to the immediate superior and centered to the midpoint of the Gaussian fit.

3.4. Expression of Results

A logarithmic regression of the wideband values and speeds is performed to build a model which predicts the behavior of the noise emission. The reference speed applied to the regression is in accordance with the speed limit of the test site, e.g., 50 km/h. A linear logarithmic plot is used to represent the regression with SEL_{speed} and L_{Amax} values. Figure 7 shows the regression of the measured values and the predicted curve of the model. The global result, presented inside the box, contains the predicted value at 50 km/h with an expanded uncertainty with 95% confidence. In addition, one of the combined uncertainties is related to the standard error of the intersection of the curve and the reference speed, and Type B instrumentation uncertainties were considered.

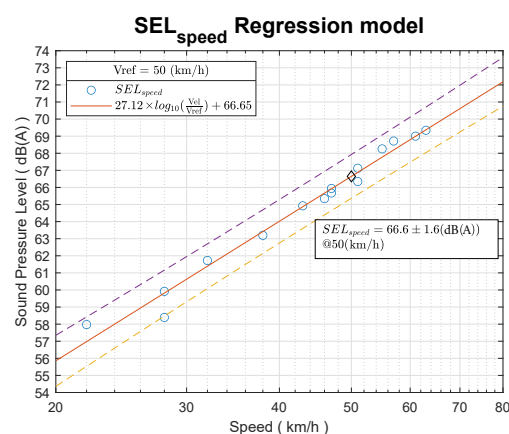


Figure 7. SEL_{speed} logarithmic linear regression of an EV measurement session. The regression red curve is also represented by the formula inside the legend box, and the two dashed lines describe the confidence interval of the fit model.

The text box over the plot indicates the value of the black diamond symbol, i.e., SEL_{speed} at 50 km/h, including its uncertainty. The red curve represents the prediction of the logarithmic regression, and the dashed lines correspond to the confidence interval of the model.

In accordance with the practical measurement correction applied in the French norm [50], for the variability of weather conditions we refer to $\theta_{ref} = 20\text{ }^{\circ}\text{C}$ as a reference temperature, $SEL_{@RefSpeed}$ corresponds to the value of the curve at the reference speed, and we use a factor of $\kappa = 0.1\text{ dB}/^{\circ}\text{C}$. Thus, the weather correction calculation is determined by Equation (4).

$$SEL_{speed} = SEL_{@RefSpeed} + \kappa(\theta - \theta_{ref}) \quad (4)$$

4. Discussion

The double Gaussian fitted model was subjected to analysis in order to compare the portion of energy considered by SEL_{speed} and the traditional SEL_{10dB} . The evaluation of the exposure level is tightly related to the duration of the pass-by, even though both parameters estimate their periods in two different modes. For instance, Figure 8 displays a complete session of passages which corresponds to the linear regression plot depicted previously in Figure 7.

Each subplot graphic shows the passages, with the speed value in the header. This demonstrates the effective relationship of reducing the portion of the signal in time and space. Furthermore, L_{Amax} is printed over the signal with a diamond symbol. Even though signals are shorter while the passage speed increases, the signal shape continues to be correctly fitted by the double Gaussian function.

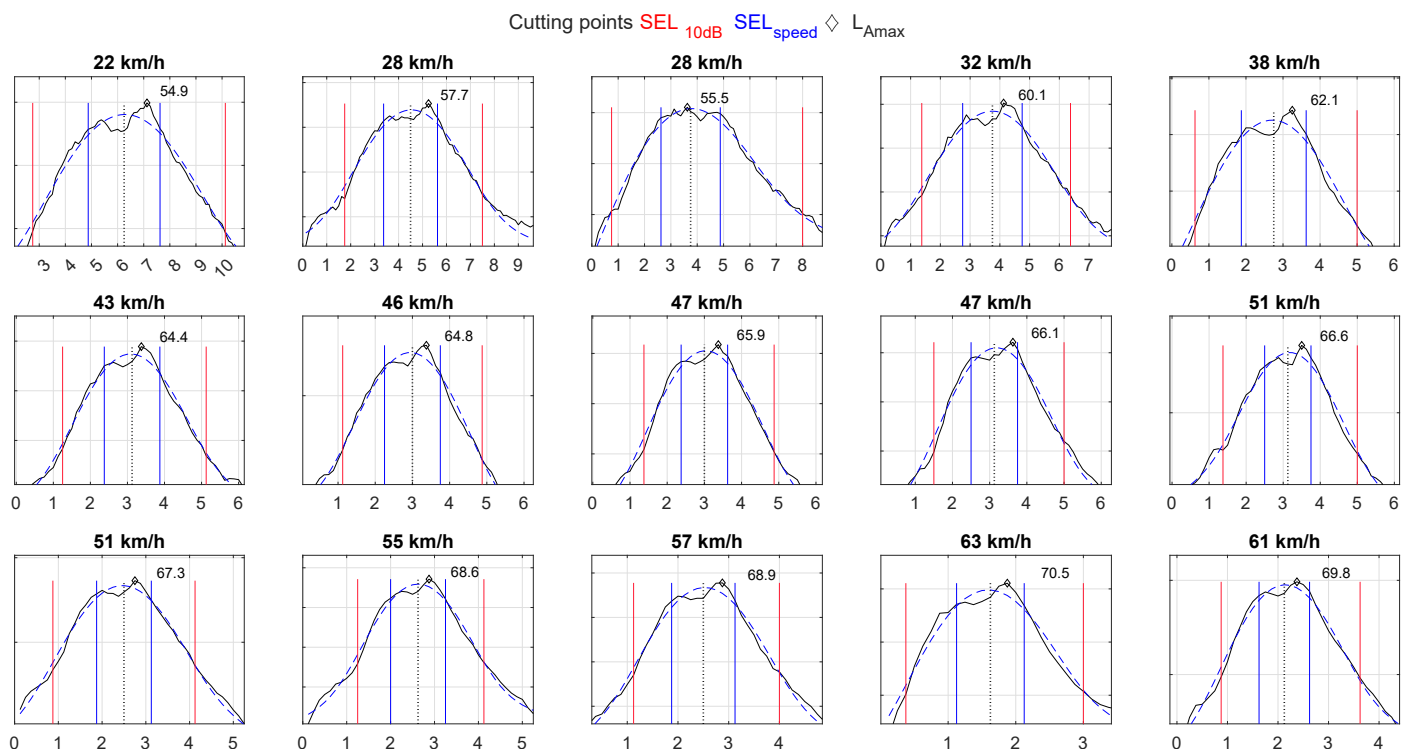


Figure 8. Signals of a complete measurement session. Red and blue vertical lines indicate the cutting points of the integration temporal window for SEL_{10dB} and SEL_{speed} , respectively.

In detail, the ordinate corresponds to the time domain in seconds and abscissa for the sound pressure level in dB(A); the red and blue vertical lines are the cutting points of the signal for SEL_{10dB} and SEL_{speed} , respectively; L_{Amax} is marked with a black diamond, and its value is written over each plot; and the black vertical dotted line corresponds to the maximum point of the double Gaussian fit.

The SEL_{speed} temporal window is moved and centered symmetrically with respect to the SEL_{10dB} region, and its size is adjusted with increasing speed. While SEL_{10dB} could be calculated by simply integrating the recorded sound levels within the period in which a decrease of 10 dB is observed, this procedure can only be performed for measurements carried out in large test sites where the region of evaluation and the hemisphere exceeds approximately three times that proposed for the SEL_{speed} . This new parameter brings up the reduction of the road segment. This shorter portion of road allows the direct sound to be collected in far field conditions, and avoids the need to consider possible shadow attenuation and/or reflection contributions caused by nearby surfaces.

The third sample, at 28 km/h, depicts a longer SEL_{10dB} temporal window compared to the rest of the samples. In consequence, this difference in window size allows for confirmation of outliers, as can be observed in Figures 7 and 9. Other examples of repeatability of the method are at 47 km/h and 51 km/h, where the greatest difference is less than 0.7 dB(A). Note that the confidence interval of the regression, on which the global result is based, depends on the correct selection and discarding of the signals.

A spectral analysis was performed in order to identify the energy contribution to L_{Amax} of every frequency band. By means of spectrograms, it was observed that the SEL_{speed} temporal window takes into account the maximum noise level of the majority of frequency bands. For instance, Figure 9 illustrates the energy distribution and its noise generation according to the speed increase; the X axis corresponds to the time domain in seconds, and 24 third-octave bands are distributed along the Y axis. The frequency domain ranges from 50 Hz to 10 kHz, from the bottom up, while the subplots correspond to the same measurement session detailed in Figures 7 and 8.

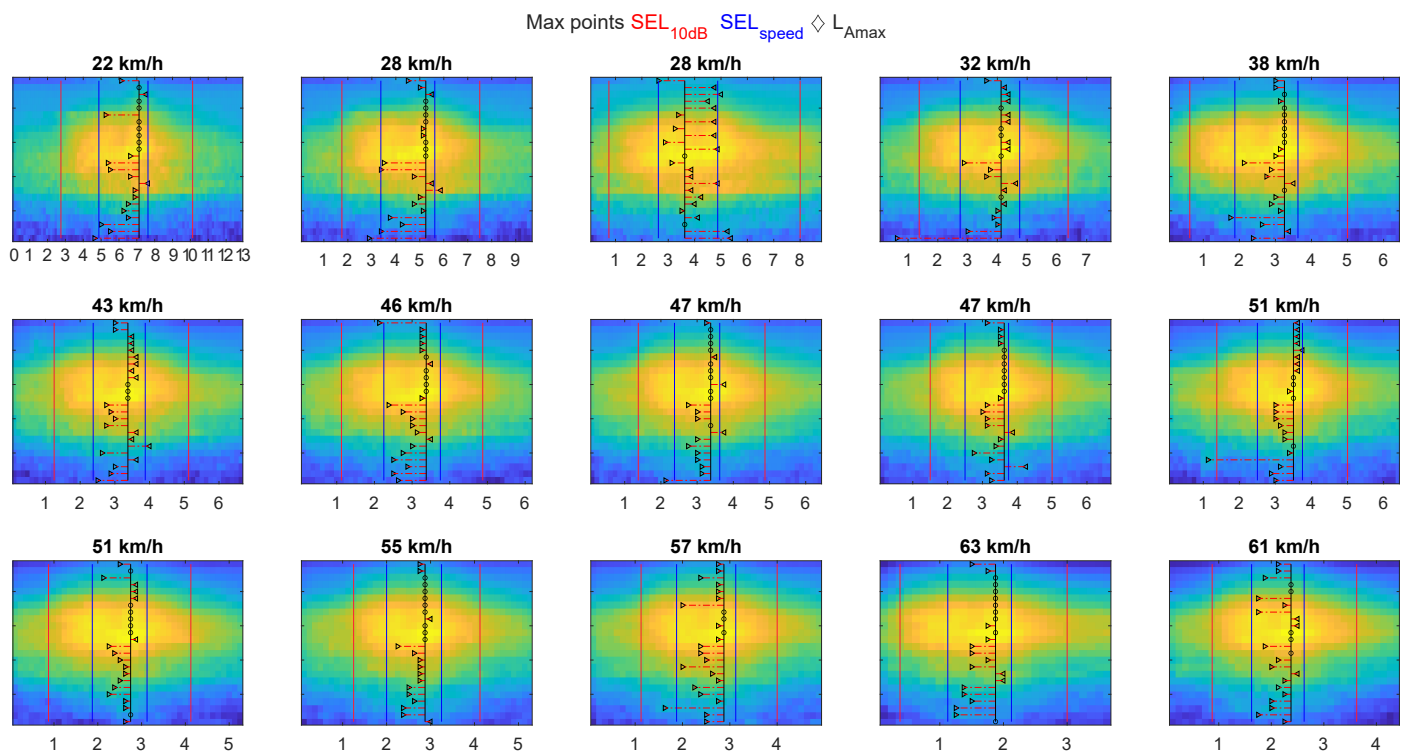


Figure 9. Spectrograms of a measurement session. Red and blue vertical lines indicate the cutting points of the integration temporal window for SEL_{10dB} and SEL_{speed} , respectively.

Again, the red and blue vertical lines are the cutting points of the signal for SEL_{10dB} and SEL_{speed} , respectively, the black triangles illustrate the L_{Amax} position of every third octave band, and the black vertical line indicates the sample position of L_{Amax} in wideband.

Remarkably, the L_{Amax} wideband instants do not correspond to the same sample positions of every third octave band, nor do they correspond to the closest source/receiver moment. Nevertheless, these peaks of energy are considered within the length of the proposed fifteen-meter region, where most of the energy of the passage is concentrated.

In wideband, identification of outliers cannot be easily accomplished, as no notable particularity can be observed. Outlier recognition is achieved by spotting the time delay along the third octave bands, especially for mid–high frequencies. For instance, the third sample in Figures 7–9 at 28 km/h shows a clear scattered distribution of black triangles, and a clear unbalanced shift in the time delay is visible from 800 Hz to 6.3 kHz. Thus, it can be assumed that the vehicle’s pass-by emission is being masked by other noise sources.

As the sound generation mechanisms that occur during vehicle’s pass-by involve more than just the tire-road interaction, they contribute to both the energy level and the frequency response. Among these sources, the most accountable are the turbine for propulsion, friction produced by front/rear wheels being driven, airflow interaction with the bodywork, etc. In EVs, thermal engine noise is absent; however, there are several systems that may operate situationally, as well as the Acoustic Vehicle Alerting System (AVAS) speaker, which is active at low speeds as required by international regulations.

5. Conclusions

Controlled Pass-By (CPB) is a widely used measurement method for evaluating noise emitted by road infrastructure, and particularly to assess the overall acoustic performance of sustainable road pavement through clear and repeatable measurements. The standard CPB procedure evaluates the A-weighted maximum level (L_{Amax}) of a vehicle’s pass-by acquired in an environment without obstacles and undesired sound sources other than the vehicle itself. While this allows very precise evaluation of the noise generated by a particular vehicle due to its tire set interacting with the pavement, the standard CPB method is not very well suited for application in urban environments. Moreover, the L_{Amax} metric does not provide all relevant information about a vehicle passage, making it not directly suitable for evaluating the total emission energy. This last aspect is evident when trying to use CPB results as input for noise maps.

An adjusted CPB has been proposed in the present work with the aim to overcome the limitations of the standard approach. This adjusted method represents a useful urban planning instrument from both the project and validation points of view. The proposed method was tested in actual urban conditions and applied to speeds ranging from 20 km/h to 70 km/h, which are typical speeds for such environments. This extends the typical range allowed by the standard CPB, which is restricted to speeds above 60 km/h. The measurement protocol is similar to the standard technique, with at least one microphone placed 7.5 m from the center of the evaluated lane. A number of technical adjustments are summarized; markings are delineated directly on the surface to guide the driver in order to support the repeatability of the trajectory during each passage and to avoid of unwanted road elements such as manhole covers and speed bumps. An acceleration segment of road before the measuring zone is set to allow the maximum target speed to be reached. The point on the travelling path nearest to the microphone is placed at the center of a hemisphere with 15 m radius, inside which no significant obstacles must be present. The passage speed is measured using suitable equipment.

Most of our proposed improvements concern the analysis phase, where we move beyond the standard technique through the (SEL_{speed}) metric. The pass-by pressure level is integrated over a constant road section or for a duration that is inversely proportional to the passage speed. In this way, unavoidable road elements such as speed cushions or manhole covers can be excluded from the analysis in most cases. Semi-automatic recognition of a passage is possible thanks to a double Gaussian fitted model, allowing the acoustic center of the passage to be evaluated, around which the cut is performed to integrate the (SEL_{speed}) calculation. Moreover, this approach allows for confirmation that there is not excessive background noise disturbing a specific passage. The (SEL_{speed}) metric shows a

linear dependence on the logarithm of the speed, confirming the validity, scalability, and most importantly, the comparability of results obtained at different test sites with respect to the technique conditions.

Finally, we proposed and validated a tool to find outliers in the log-linear fit by analyzing the time of arrival of the maximum levels in each third-octave frequency band with respect to the position of the passage's (L_{Amax}) metric. This is clearly observable thanks to a spectrographic representation of the passages defined in the present work.

Future developments include the use of the adjusted CPB procedure to characterize sound emissions in an ideal and optimistic situation comprising a fleet of EVs, silent tires, and optimized pavement. Extensive measurement campaigns have already been carried out on selected test sites as part of the Life E-VIA Project, with an analysis performed following our new proposed methodology. Comparing these measurements can provide support for the definition of standardized reference values for the SEL_{speed} index. The proposed measurement protocol can be used in two of the most prominent open problems in environmental acoustics, namely, the assessment of low noise emission road pavement types and the description of the sound emissions associated with EVs. These aspects intersect with other open problems pertaining to the preservation of the urban environment, and might lead to the development of effective and sustainable solutions. Finally, the proposed methodology can act as the basis for acquiring the data needed to calculate CNOSSOS-EU coefficients for the fifth open category, which is the aim of our upcoming work.

Author Contributions: Conceptualization, R.M.; Data curation, F.B. and S.C.; Formal analysis, R.M., S.C. and A.M.; Funding acquisition, G.L.; Investigation, F.B., A.M. and L.F.; Methodology, R.M., A.M. and L.F.; Project administration, G.L.; Resources, F.B.; Software, R.M. and S.C.; Supervision, F.B., L.F. and G.L.; Validation, F.B. and L.F.; Writing—original draft, R.M., A.M. and L.F.; Writing—review and editing, F.B., S.C., L.F. and G.L. All authors have read and agreed to the published version of the manuscript.

Funding: This research was funded by the European Commission under the program Life Environment and Resource Efficiency: LIFE18 ENV/IT/000201—“Electric Vehicle noise control by Assessment and optimisation of tyre/road interaction.”

Informed Consent Statement: Not applicable.

Data Availability Statement: The data that support the findings of this study are available in this paper.

Conflicts of Interest: The authors declare no conflict of interest.

Abbreviations

The following abbreviations are used in this manuscript:

RTN	Road Traffic Noise
EVs	Electric Vehicles
GPP	Green Public Procurement Criteria
CPX	Close Proximity Index
SPB	Statistical Pass-By
CPB	Controlled Pass-By

References

1. Peris, E. Environmental noise in Europe: 2020. *Eur. Environ. Agency* **2020**, *1*, 104.
2. Themann, C.L.; Masterson, E.A. Occupational noise exposure: A review of its effects, epidemiology, and impact with recommendations for reducing its burden. *J. Acoust. Soc. Am.* **2019**, *146*, 3879–3905. [[CrossRef](#)]
3. Axelsson, A.; Prasher, D. Tinnitus induced by occupational and leisure noise. *Noise Health* **2000**, *2*, 47.
4. Pienkowski, M. Loud music and leisure noise is a common cause of chronic hearing loss, tinnitus and hyperacusis. *Int. J. Environ. Res. Public Health* **2021**, *18*, 4236. [[CrossRef](#)] [[PubMed](#)]
5. Basner, M.; Babisch, W.; Davis, A.; Brink, M.; Clark, C.; Janssen, S.; Stansfeld, S. Auditory and non-auditory effects of noise on health. *Lancet* **2014**, *383*, 1325–1332. [[CrossRef](#)] [[PubMed](#)]

6. Waye, K.P.; van Kempen, E. Non-auditory effects of noise: An overview of the state of the science of the 2017–2020 period. In Proceedings of the International Commission on Biological Effects of Noise, Stockholm, Sweden, 14–17 June 2021.
7. Thompson, R.; Smith, R.B.; Karim, Y.B.; Shen, C.; Drummond, K.; Teng, C.; Toledano, M.B. Noise pollution and human cognition: An updated systematic review and meta-analysis of recent evidence. *Environ. Int.* **2022**, *158*, 106905. [[CrossRef](#)] [[PubMed](#)]
8. Schubert, M.; Hegewald, J.; Freiberg, A.; Starke, K.R.; Augustin, F.; Riedel-Heller, S.G.; Zeeb, H.; Seidler, A. Behavioral and emotional disorders and transportation noise among children and adolescents: A systematic review and meta-analysis. *Int. J. Environ. Res. Public Health* **2019**, *16*, 3336. [[CrossRef](#)]
9. Guski, R.; Schreckenber, D.; Schuemer, R. WHO environmental noise guidelines for the European region: A systematic review on environmental noise and annoyance. *Int. J. Environ. Res. Public Health* **2017**, *14*, 1539. [[CrossRef](#)]
10. Basner, M.; McGuire, S. WHO environmental noise guidelines for the European region: A systematic review on environmental noise and effects on sleep. *Int. J. Environ. Res. Public Health* **2018**, *15*, 519. [[CrossRef](#)]
11. Dzhambov, A.M.; Lercher, P. Road traffic noise exposure and depression/anxiety: An updated systematic review and meta-analysis. *Int. J. Environ. Res. Public Health* **2019**, *16*, 4134. [[CrossRef](#)]
12. Petri, D.; Licitra, G.; Vigotti, M.A.; Fredianelli, L. Effects of exposure to road, railway, airport and recreational noise on blood pressure and hypertension. *Int. J. Environ. Res. Public Health* **2021**, *18*, 9145. [[CrossRef](#)] [[PubMed](#)]
13. Van Kempen, E.; Casas, M.; Pershagen, G.; Foraster, M. WHO environmental noise guidelines for the European region: A systematic review on environmental noise and cardiovascular and metabolic effects: A summary. *Int. J. Environ. Res. Public Health* **2018**, *15*, 379. [[CrossRef](#)]
14. Lim, S.S.; Vos, T.; Flaxman, A.D.; Danaei, G.; Shibuya, K.; Adair-Rohani, H.; AlMazroa, M.A.; Amann, M.; Anderson, H.R.; Andrews, K.G.; et al. A comparative risk assessment of burden of disease and injury attributable to 67 risk factors and risk factor clusters in 21 regions, 1990–2010: A systematic analysis for the Global Burden of Disease Study 2010. *Lancet* **2012**, *380*, 2224–2260. [[CrossRef](#)] [[PubMed](#)]
15. Locher, B.; Piquerez, A.; Habermacher, M.; Ragetti, M.; Rösli, M.; Brink, M.; Cajochen, C.; Vienneau, D.; Foraster, M.; Müller, U.; et al. Differences between outdoor and indoor sound levels for open, tilted, and closed windows. *Int. J. Environ. Res. Public Health* **2018**, *15*, 149. [[CrossRef](#)]
16. Olafsen, S. Sound insulation against traffic noise in wooden houses. In Proceedings of the BNAM, Lyngby, Denmark, 20–23 May 2002.
17. Easteal, M.; Bannister, S.; Kang, J.; Aletta, F.; Lavia, L.; Witchel, H. Urban sound planning in Brighton and Hove. In Proceedings of the Forum Acusticum, Krakow, Poland, 7–12 September 2014; pp. 7–12.
18. Cerwén, G.; Mossberg, F. Implementation of quiet areas in Sweden. *Int. J. Environ. Res. Public Health* **2019**, *16*, 134. [[CrossRef](#)]
19. Tiboni, M.; Rossetti, S.; Vetturi, D.; Torrisi, V.; Botticini, F.; Schaefer, M.D. Urban policies and planning approaches for a safer and climate friendlier mobility in cities: Strategies, initiatives and some analysis. *Sustainability* **2021**, *13*, 1778. [[CrossRef](#)]
20. Corticelli, R.; Pazzini, M.; Mazzoli, C.; Lantieri, C.; Ferrante, A.; Vignali, V. Urban Regeneration and Soft Mobility: The Case Study of the Rimini Canal Port in Italy. *Sustainability* **2022**, *14*, 14529. [[CrossRef](#)]
21. Heutschi, K.; Bühlmann, E.; Oertli, J. Options for reducing noise from roads and railway lines. *Transp. Res. Part Policy Pract.* **2016**, *94*, 308–322. [[CrossRef](#)]
22. Heutschi, K.; Locher, B.; Gerber, M. sonROAD18: Swiss implementation of the CNOSSOS-EU road traffic noise emission model. *Acta Acust. United Acust.* **2018**, *104*, 697–706. [[CrossRef](#)]
23. Ohiduzzaman, M.; Sirin, O.; Kassem, E.; Rochat, J.L. State-of-the-art review on sustainable design and construction of quieter pavements—Part 1: Traffic noise measurement and abatement techniques. *Sustainability* **2016**, *8*, 742. [[CrossRef](#)]
24. Sandberg, U.; Ejsmont, J. *Tyre/Road Noise. Reference Book*; INFORMEX Ejsmont & Sandberg: Kisa, Sweden, 2002.
25. Kuijpers, A.; Van Blokland, G. Tyre/road noise models in the last two decades: A critical evaluation. In Proceedings of the INTER-NOISE and NOISE-CON Congress and Conference Proceedings, The Hague, The Netherlands, 27–30 August 2001; Institute of Noise Control Engineering: Washington, DC, USA, 2001; Volume 2001, pp. 2494–2499.
26. Vasilyev, A. About the approaches to mathematical description and calculation of tire road noise radiation. *Akustika* **2019**, *32*, 97–99. [[CrossRef](#)]
27. Ling, S.; Yu, F.; Sun, D.; Sun, G.; Xu, L. A comprehensive review of tire-pavement noise: Generation mechanism, measurement methods, and quiet asphalt pavement. *J. Clean. Prod.* **2021**, *287*, 125056. [[CrossRef](#)]
28. Del Pizzo, L.; Teti, L.; Moro, A.; Bianco, F.; Fredianelli, L.; Licitra, G. Influence of texture on tyre road noise spectra in rubberized pavements. *Appl. Acoust.* **2020**, *159*, 107080. [[CrossRef](#)]
29. de León, G.; Del Pizzo, L.G.; Teti, L.; Moro, A.; Bianco, F.; Fredianelli, L.; Licitra, G. Evaluation of tyre/road noise and texture interaction on rubberised and conventional pavements using CPX and profiling measurements. *Road Mater. Pavement Des.* **2020**, *21*, S91–S102. [[CrossRef](#)]
30. Jaiswal, S.; Sharma, S. Electric vehicles and smart grid interactions: Infrastructure, current trends, impacts and challenges. In *Smart Grids for Renewable Energy Systems, Electric Vehicles and Energy Storage Systems*; CRC Press: Boca Raton, FL, USA, 2023; pp. 15–44.
31. Pallas, M.A.; Berengier, M.; Chatagnon, R.; Czuka, M.; Conter, M.; Muirhead, M. Towards a model for electric vehicle noise emission in the European prediction method CNOSSOS-EU. *Appl. Acoust.* **2016**, *113*, 89–101. [[CrossRef](#)]

32. (EAFO European Alternative Fuels Observatory Alternative Fuels Vehicles Share. 2022. Available online: <https://alternative-fuels-observatory.ec.europa.eu/> (accessed on 30 January 2023).
33. Melloni, A.; Pecchioni, G.; Luzzi, S.; Bellomini, R. Life E-via Project: Noise, Electric Vehicles and Tyres. 2020; p. 13. Available online: <https://hal.science/hal-03233738> (accessed on 28 January 2023).
34. Yamauchi, K.; Yabuno, M.; Yamasaki, R. Sound power level of electric vehicles running in steady low speed. *Acoust. Sci. Technol.* **2020**, *41*, 626–629. [[CrossRef](#)]
35. Campello-Vicente, H.; Peral-Orts, R.; Campillo-Davo, N.; Velasco-Sanchez, E. The effect of electric vehicles on urban noise maps. *Appl. Acoust.* **2017**, *116*, 59–64. [[CrossRef](#)]
36. Jabben, J.; Verheijen, E.; Potma, C. Noise reduction by electric vehicles in the Netherlands. In Proceedings of the INTER-NOISE and NOISE-CON Congress and Conference Proceedings, New York, NY, USA, 19–22 August 2012; Institute of Noise Control Engineering: Washington, DC, USA, 2012; Volume 2012, pp. 6958–6965.
37. Vaitkus, A.; Čygas, D.; Vorobjovas, V.; Andriejauskas, T. Traffic/road noise mitigation under modified asphalt pavements. *Transp. Res. Procedia* **2016**, *14*, 2698–2703. [[CrossRef](#)]
38. Li, B.; Cao, K.; Zhou, J.; Li, A.; Sun, M. Laboratory investigation on influence of mixture parameters on noise reduction characteristics of porous asphalt concrete. *Int. J. Pavement Eng.* **2022**, 1–15. [[CrossRef](#)]
39. Licitra, G.; Moro, A.; Teti, L.; Del Pizzo, L.; Bianco, F. Modelling of acoustic ageing of rubberized pavements. *Appl. Acoust.* **2019**, *146*, 237–245. [[CrossRef](#)]
40. Praticò, F.G.; Pellicano, G.; Fedele, R. Low-noise road mixtures for electric vehicles. In Proceedings of the Euronoise 2021 Conference, Madeira, Portugal, 21–23 June 2021; pp. 25–27.
41. Garbarino, E.; Quintero, R.R.; Donatello, S.; Wolf, O. *Revision of Green Public Procurement Criteria for Road Design, Construction and Maintenance. Procurement Practice Guidance Document*; Office of the European Union: Luxembourg, 2016.
42. *EN ISO 11819-1; Acoustics—Measurement of the Influence of Road Surfaces on Traffic Noise—Part 1: Statistical Pass-By Method*. The International Organization for Standardization: Geneva, Switzerland, 1997.
43. Mikhailenko, P.; Piao, Z.; Kakar, M.R.; Bueno, M.; Athari, S.; Pieren, R.; Heutschi, K.; Poulikakos, L. Low-Noise pavement technologies and evaluation techniques: A literature review. *Int. J. Pavement Eng.* **2022**, *23*, 1911–1934. [[CrossRef](#)]
44. Ganji, M.R.; Ghelmani, A.; Golroo, A.; Sheikhzadeh, H. Mean texture depth measurement with an acoustical-based apparatus using cepstral signal processing and support vector machine. *Appl. Acoust.* **2020**, *161*, 107168. [[CrossRef](#)]
45. Knabben, R.M.; Triches, G.; Vergara, E.F.; Gerges, S.N.; van Keulen, W. Characterization of tire-road noise from Brazilian roads using the CPX trailer method. *Appl. Acoust.* **2019**, *151*, 206–214. [[CrossRef](#)]
46. Ramos-Romero, C.; Asensio, C.; Moreno, R.; de Arcas, G. Urban Road Surface Discrimination by Tire-Road Noise Analysis and Data Clustering. *Sensors* **2022**, *22*, 9686. [[CrossRef](#)]
47. de Vos, P.; Beuving, M.; Verheijen, E. Harmonised accurate and reliable methods for the EU directive on the assessment and management of environmental noise—Final technical report. *Tek. Rapp.* **2005**, *22*. Available online: <https://cordis.europa.eu/project/id/IST-2000-28419> (accessed on 28 January 2023).
48. *IMAGINE Improved Methods for the Assessment of the Generic Impact of Noise in the Environment*; IMAGINE Projec FP6 CORDIS; European Commission: Brussels, Belgium, 2012.
49. Ascari, E.; Cerchiai, M.; Fredianelli, L.; Licitra, G. Statistical Pass-By for Unattended Road Traffic Noise Measurement in an Urban Environment. *Sensors* **2022**, *22*, 8767. [[CrossRef](#)]
50. *NF S31-119-2:2000; Acoustics—In Situ Characterization of the Acoustic Qualities of Road Surfaces—Pass by Acoustic Measurement—Part 2: Controlled Pass-by Method*. Afnor: Paris, France, 2000.
51. Clar-Garcia, D.; Velasco-Sanchez, E.; Campillo-Davo, N.; Campello-Vicente, H.; Sanchez-Lozano, M. A new methodology to assess sound power level of tyre/road noise under laboratory controlled conditions in drum test facilities. *Appl. Acoust.* **2016**, *110*, 23–32. [[CrossRef](#)]
52. Ho, K.Y.; Hung, W.T.; Ng, C.F.; Lam, Y.K.; Leung, R.; Kam, E. The effects of road surface and tyre deterioration on tyre/road noise emission. *Appl. Acoust.* **2013**, *74*, 921–925. [[CrossRef](#)]
53. Ji, H.; Zhang, M.; Kim, B.S. Parameter conversion between controlled pass-by method and alternative close proximity method. *Appl. Sci.* **2020**, *10*, 5679. [[CrossRef](#)]
54. Licitra, G.; Teti, L.; Bianco, F.; Chetoni, M.; Ascari, E. Relationship between Pass By results, CPX ones and roadside long-term measures: Some considerations. In Proceedings of the INTER-NOISE and NOISE-CON Congress and Conference Proceedings, Hamburg, Germany, 21–24 August 2016; Institute of Noise Control Engineering: Washington, DC, USA, 2016; Volume 253, pp. 2508–2516.
55. Dhamaniya, A.; Chandra, S. Speed prediction models for urban arterials under mixed traffic conditions. *Procedia-Soc. Behav. Sci.* **2013**, *104*, 342–351. [[CrossRef](#)]
56. Praticò, F.G.; Giunta, M. Quantifying the effect of present, past and oncoming alignment on the operating speeds of a two-lane rural road. *Balt. J. Road Bridge Eng.* **2012**, *7*, 181–190. [[CrossRef](#)]
57. Praticò, F.G.; Giunta, M. Speed distribution on low-volume roads in Italy: From inferences to rehabilitation design criteria. *Transp. Res. Rec.* **2011**, *2203*, 79–84. [[CrossRef](#)]

58. Bokare, P.S.; Maurya, A.K. Acceleration-deceleration behaviour of various vehicle types. *Transp. Res. Procedia* **2017**, *25*, 4733–4749. [[CrossRef](#)]

Disclaimer/Publisher's Note: The statements, opinions and data contained in all publications are solely those of the individual author(s) and contributor(s) and not of MDPI and/or the editor(s). MDPI and/or the editor(s) disclaim responsibility for any injury to people or property resulting from any ideas, methods, instructions or products referred to in the content.